A dual marker label free electrochemical assay for *Flavivirus* dengue diagnosis

Adriano Santos[1], Paulo R. Bueno[1]* and Jason J. Davis[2#]

[1]Physical Chemistry Department, Institute of Chemistry, São Paulo State University, (Univ. Estadual Paulista, UNESP), Nanobionics group (www.nanobionics.pro.br), CEP: 14800-060, Araraquara, São Paulo, Brazil.
[2]Department of Chemistry, University of Oxford, South Parks Road, Oxford OX1 3QZ, United Kingdom

Corresponding authors:
*Paulo R. Bueno. Physical Chemistry Department, Institute of Chemistry. São Paulo State University (Univ. Estadual Paulista, UNESP). Nanobionics research group (www.nanobionics.pro.br).CEP: 14800-060, Araraquara, São Paulo, Brasil.
prbueno@iq.unesp.br
Tel: +55 16 3301 9642, Fax: +55 16 3322 2308

#Jason J. Davis
Department of Chemistry, University of Oxford, South Parks Road, Oxford, OX1 3QX, UK
Jason.davis@chem.ox.ac.uk

Abstract

Dengue is a RNA viral illness of the genus *Flavivirus* which can cause, depending on the pervasiveness of the infection, hemorrhagic dengue fever likewise known as dengue shock syndrome. Herein we present an electrochemical label free approach enabling the rapid sensitive quantification of NS1 and IgG (a tool supporting an ability to distinguish primary and secondary infections). Using a bifunctional SAM containing PEG moieties and tethered redox thiol, both markers are detectable across clinically relevant levels by label free impedance spectroscopy derived redox capacitance. A subsequent frequency specific immittance function approach enables even more rapid assaying (within seconds) with no impairment of analytical parameters (such as linearity, sensitivity and variance).

Keywords: molecular diagnostics, biosensor, electrochemical capacitance spectroscopy, electrochemical immittance analysis, dengue, NS1, IgG.

1. Introduction

Dengue is an infection caused by RNA virus (DENV), a member of *Flavivirus* genus. [1] DENV virus has four different serotypes (DENV1, DENV2, DENV3 and DENV4) which can cause, depending on the incidence (first or secondary infection), [2, 3] dengue fever (DF) or dengue hemorrhagic fever (DHF) alternatively known as dengue shock syndrome (DSS) [2]. The symptoms vary from little physical prognosis to a severe disease status as characterized by bleeding and circulatory failure. Dengue is transmitted from one person to another by the bites [2] of a female contaminated *Aedes* mosquito, [4] which propagates in urban areas in subtropical and tropical regions. [2] Frequently outbreaks are reported in Asia-Pacific region, both central and south America and southeast of the Gulf of Mexico. [2] In Brazil alone, over a million cases of dengue were registered from January to May of 2015 and, in 2016, an increase of about 50% was registered in the first two months of the year, over 2015 levels. Epidemics have additionally been reported in 2010 in Philippines, Caribbean, Central America and Sri Lanka. [2] It is important to highlight that, due to climate changes [5] and an increase in global travelling, [1] dengue re-emerged in 2009 in Florida [2] and an outbreak in 2012 was reported in Portugal, the first since the 1920s. [6] It is now considered a global public health issue [7] where 3.6 billion people over 124 countries are estimated to be at-risk of infection. [8] In view of this scale, and in the absence of efficient vaccines or therapeutics, [4] rapid, accurate and practical diagnosis enabling immediate patient management and a control of spread is of considerable value. [3]

Virus isolation and cultivated in vitro followed by an immunofluorescence assay is considered the “gold standard” approach for dengue detection. [1, 2] Though highly specific, the methodology requires a long incubation time (7-12 days) and lab facilities with skilled personnel. [1] In addition, the appropriate window for virus culturing is limited to up seven days following the onset of symptoms, making this methodology impractical for routine screening. [1] Diagnosis based on RNA detection by reverse transcription polymerase chain reaction (RT-PCR) is used for detecting the viral RNA and, again, though specificity is high, this is a costly, laborious and time intensive process, [1, 2, 4]. The latter consist of an approximately three-hour-procedure [9] involving RNA isolation, the production of a single-strand complementary DNA copy, PCR amplification, separation, detection and quantification by optical [10] or electrochemical [11] measurements. PCR methods are, additionally, only effective shortly after disease onset [2] and suffer from false-positives through cross-contamination with dengue virus PCR products in the laboratory. Serological tests such as MAC-ELISA (monoclonal antibody capture-enzyme linked immunosorbent assay), [2] are not

accessible in resource-limited healthcare settings nor remotely portable (enzyme labeled secondary antibodies, repetitive incubation steps and UV-VIS readout are required). [2, 4] Electroanalytical methods offer much to deal with challenges involving sensitivity, portability and additionally can be both rapid and label free. [12, 13]

Recent studies have shown that non-structural protein 1 (NS1) can be used as a biomarker for detection of dengue. [14-16] NS1 is a ~45 KDa glycoprotein [17] expressed in infected cells and can be detected within a week of symptom onset in a concentration range of 0.04-2.00 μg/mL in serum of primary infected patients and 0.01-2.00 μg/mL in secondary one. [15] There are additional reports that a combined detection of NS1 antigen and its antibodies (IgM and/or IgG) improves diagnostic sensitivity and aids the identification of secondary infections, critical in detecting likely severe forms of this disease. [18, 19] NS1 represents an early stage biomarker, [15] with IgM detection possible to be detected from the third day after contamination, persisting for approximately three months. [20] IgG levels spike 5-14 days after contamination. [20, 21] In secondary infections, however, the IgG titer increases within 1-2 days to levels that are several orders of magnitude higher than observed prior to infection. [21] IgG analysis thus can be used as confirmatory of secondary infection where IgM is less so. [19, 20] (see supplementary material-section S1, SM-S1).

To date a number of low cost diagnostic platforms for NS1 (and also combined with IgG and IgM) have been reported, including those based on impedimetric analyses. [1, 4, 22-28] For example, Cecchetto et al. [26] have reported an impedimetric biosensor to detect NS1 both in PBS and serum using a surface tethered anti-NS1 antibody. Similarly, Darwish et al. [27] have reported an impedance immunosensor for NS1 detection through the multistep construction of an immobilized gold nanoparticle-anti-NS1 antibody film. Traditional impedimetric (faradaic or non-faradaic) approaches are inherently spectroscopic, with data acquisition typically across a broad range of applied AC frequencies (1 MHz to 10 mHz) prior to subsequent fitting of experimental data to a convenient electric circuit. [13] In the dominant faradaic approach, it is additionally necessary to pre-dope with an amplifying excess of redox probe [29] prior using the resolved charge transfer resistance (R_{ct}) as signal transduction. As an alternative, we have introduced the use of redox tagged receptor interfaces and redox capacitance (C_r) (from electrochemical impedance-derived capacitance spectroscopy) as underpinning a fully label free sensory approach. [30-32] Although this approach brings significant practical advantages, by default, it also requires a full spectrum analysis. We have also introduced an immittance function methodology that enables a more facile

analysis without any data fitting.[32, 33] The concept is based on the relationship between potential perturbation and measured current being described by mathematically exchangeable complex immittance functions (e.g. impedance Z*, capacitance C*, admittance Y* and modulus M*). It is possible, within this, to obtain different transduction signals using only one data set without any reference to equivalent circuits. [32-34] The benefit of using immittance function approach is that it is, in essence, a "plug and play" concept wherein sensor "chip" is coupled to the read out device, allowing to set up an algorithm which searches for the most sensitive function with correspondent frequency or narrow range of frequencies. In previous work we have demonstrated this application to a number of markers. [32-34]

Presently we expand this approach to Dengue diagnostics using molecular self-assembled monolayer (SAM) and compare both redox capacitance and immittance function methods. SAM was constructed onto gold surface using two different thiols: 11-ferrocenylundenethiol, for target detection, and PEG-thiol (with low fouling features) [35], for recognition coupling element. Using this bifunctional SAM (with low fouling characteristic and yet redox tagged characteristics), represent the first dual electrochemical dengue marker assay reported to date, ultimately enabling the future development of a useful routine diagnostic within seconds.

2. Experimental

2.1 Chemicals and biochemicals reagents

The chemicals described in this section were purchased from Sigma-Aldrich, except the PEG-thiol (HS-C11-EG3-OCH_2-COOH, EG = ethylene glycol) and 11-(ferrocenyl)-undecanethiol (11Fc) which were obtained from Prochimia [purity > 95%]. Non-structural protein 1 (NS1) and IgG antibody (anti-NS1, reactive for the four different dengue virus [I-IV]) were purchased from Abcam. Solutions of anti-NS1, NS1 and bovine serum albumin (BSA) 1 mg/mL were prepared in phosphate buffered saline (PBS) pH 7.4 containing NaCl (137 mmol/L), KCl, 2.7 mmol/L and freshly prepared sodium phosphate (10 mmol/L). Solutions of PBS, NaOH 500 mmol/L, H_2SO_4 500 mmol/L, *N*-(3-dimethylaminopropyl)-*N´*-ethylcarbodiimide (EDC) 400 mmol/L, *N*-Hydroxysuccinimide (NHS) 100 mmol/L and sodium perchlorate ($NaClO_4$) 100 mmol/L were prepared in Milli-Q water (Millipore system with 18.2 MΩ cm at 25 °C). Mixed solutions of PEG-thiol (0.02 mmol/L) and 11Fc (2 mmol/L) were prepared in anhydrous ethanol. Commercial human serum was obtained from Sigma and used diluted in PBS at 20% (v/v).

2.2 Electrochemical measurements

All experiments were performed at room temperature (25 °C) using $NaClO_4$ electrolyte at 100 mmol/L. Cyclic voltammetry (CV) and electrochemical impedance spectroscopy (EIS) measurements were performed using an AUTOLAB potentiostat equipped with a frequency response analysis (FRA) module and the NOVA software from Metrohm. A three-electrode system was used, including the gold electrode as working electrode (1.6 mm diameter from Basi), a platinum disc as counter electrode and Ag|AgCl (3 mol/L NaCl, from ALS Co., Ltd) as reference electrode. All potentials referred in this work are relative to Ag|AgCl (3 mol/L NaCl). All solutions used in the electrochemical assays were deaerated by N_2 purging for 25 min before use.

2.3. Surface preparation and characterization

Gold electrodes were mechanically polished using 0.1 and 0.05 µm grain-sized aluminum oxide aqueous suspensions (Buehler) followed by sonication in deionized water for 15 min to remove adhered particles. CVs for electrochemical desorption (see SM-S2) were performed in NaOH 500 mmol/L, from -1.7 to -0.5 V, 400 cycles, at the scan rate of 50 mV/s. Electrochemical cleaning CV's were performed in H_2SO_4 500 mmol/L from 0.3 to 1.5 V, 500 cycles, at scan rate of 100 mV/s, followed by CV gold oxide stripping in H_2SO_4 500 mmol/L from 0.3 to 0.6 V, 10 cycles, 100 mV/s. Electroactive areas were calculated on the basis of cyclic voltammograms from the electrochemical cleaning step by integrating the cathodic peak on the last scan using a value of 482 µC/cm^2. [36, 37] The surface roughness was determined by dividing the electro-active area by the geometric area. These determinations (0.036 ± 0.009 cm^2, with a correspondent surface roughness of 1.8 ± 0.4) were used to normalize subsequent electrochemical transduction signals.

The electro-active bifunctional SAMs were constructed by immersing cleaned electrodes for 20 h at 25°C in a mixed solution containing 0.02 mmol/L PEG-thiol and 2.0 mmol/L 11Fc in anhydrous ethanol. The carboxyl group of the PEG-thiol was then activated with an aqueous solution containing EDC 200 mmol/L and NHS 50 mmol/L for 30 min. Subsequently, the electrode was washed using water, dried with nitrogen gas and immersed in either 97 µg/mL anti-NS1 solution or 10 µg/mL NS1 antigen in PBS for 1 h. Finally, the electrodes were immersed in a BSA solution (1mg/mL) for 30 min (Figure 1) and then washed with PBS and water.

After SAM formation, CV was performed from 0.0 to 0.8 V (50 cycles) at a scan rate of 100 mV/s to resolve the redox-in potential $E_{in} = (E_{ox} + E_{red})/2$, where E_{ox} and E_{red} are the oxidation and

reduction potentials peak potentials, respectively. Impedance analyses were carried out at E_{in} in a frequency range of 100 kHz to 0.1 Hz (50 frequencies logarithmically arranged), amplitude of 10 mV, after each step of the interface construction.

Electrochemical capacitance analysis was performed by determining the capacitance from raw impedance data using the relationship $C^*(\omega) = 1/i\omega Z^*(\omega)$, where ω is the angular frequency and i is the complex number $i = \sqrt{-1}$.[38] In processing $Z^*(\omega)$, it is possible to obtain both the imaginary $C'' = \varphi Z'$ and real $C' = \varphi Z''$ portions of capacitance, noting that $\varphi = 1/(\omega|Z|^2)$, where $|Z|$ is the modulus of impedance. The 11Fc coverage (Γ_{11Fc}, mol/cm^2) was calculated from $\Gamma_{11Fc} = 4C_r k_B T/eF$, where C_r is the electrochemical or redox capacitance per cm^2 (estimated by the diameter semicircle of the capacitive Nyquist plot, as detailed in references [13, 30]), k_B is the Boltzmann constant, T is the absolute temperature (293 K), F is the Faraday constant, and e is the elementary charge.[39] Γ_{11Fc} results obtained using redox capacitance were compared with those estimated from classical voltammetry, $\Gamma_{11Fc} = Q/FA$, assuming $Fc^+ + e^- \leftrightarrows Fc$ and Q is the charge obtained by the integration peak of the reduction/oxidation process after compensating for non-faradaic contributions.[40] Γ_{11Fc} redox coverage was also calculated by analysis of the voltametric current peaks resolved at different scan rates (100-700 mV/s).[41]

CV electrochemical desorption was performed in NaOH 500 mmol/L with potential ranging from -0.2 to -1.4 V at scan rate of 50 mV/s to obtain the bi-functional SAM surface coverage (Γ_{SAM}), as described elsewhere.[36]

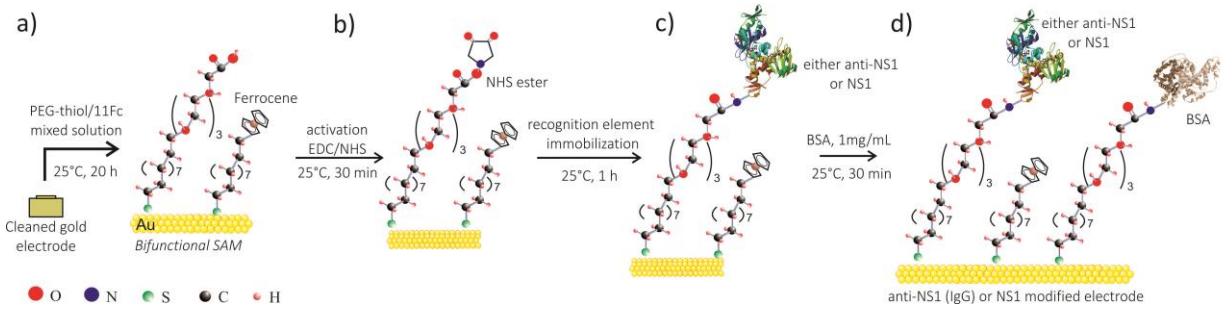

Figure 1. Schematic step by step description of the anti-NS1 and NS1 modified electrode preparations. (a) Functionalization of gold surface with a mixed solution containing 11Fc and PEG-thiol. (b) Activation of carboxylic groups prior to coupling with amino groups present in the recognition element as shown in (c). (d) Blocking non-specific sites with BSA 1mg/mL (molecules not drawn into scale).

2.4 Detection of NS1 and IgG (anti-NS1)

After the surface construction and electrochemical characterization, the functionalized electrodes were exposed for 30 min in either NS1 or IgG mAb solutions at different concentrations, ranging from 1 to 5,000 ng/mL, prepared either in PBS or diluted serum at 20% (v/v) in PBS. The electrodes were then washed with water and impedance analyses carried-out at E_{in} using $NaClO_4$ supporting electrolyte. A typical acquisition time of impedance data over the full frequency range (50 frequency points, 100,000-0.1 Hz) is approximately 4 min. All assays were carried out in triplicate and results reported as average ± standard deviation ($\bar{x} \pm sd$).

As noted above, the signal transduction (S) used herein was initially the inverse of redox capacitance (i.e. $S = 1/C_r$, where C_r is obtained from the semicircle diameter of the complex capacitance plots) and then the inverse of the imaginary part of capacitance (i.e. $S = 1/C''$). The signal transduction reported for both cases is the relative response (RR), defined as:

$$RR_{[target]}(\%) = \left[\left(S_{[target]} - S_0\right)/R_0\right]x\ 100 \qquad (1)$$

where S_0 represents the blank measurement and $S_{[target]}$ is the S value for a certain target (either NS1 or anti-NS1) concentration. Analysis of correlation coefficient (R), coefficient of determination (R^2), sensibility (slope of the linear regression in the analytical plot), limit of detection (LOD, defined as 3.3 x SD where SD means standard deviation of the blank) [42] and relative standard deviation (RSD) were performed. In order to evaluate the non-specific interactions, serum at 20% diluted in PBS was used instead of target solution. In optimizing analytical frequency for 1/C'' transduction we resolved analytical plots with a coefficient of determination $R^2 > 0.96$, with the highest sensitivity and the lowest limit of detection.

3. Results and discussion

3.1 Surface film characterization

An initial CV analysis of the 11Fc and PEG-thiol SAM (Figure 2a) resolves the expected reversible wave (peak separation 30 ± 5 mV and current peak ratio about unity (i.e. $i_{pa}/i_{pc} \approx 1$). The full width at half of the peak maximum height (FWHM), a measure of redox site homogeneity, [43] is ≈ 110 mV a little higher than the theoretical ideal for an electron process (90.6 mV),[43] but fully in line with prior reports. [41] A complete impedance characterization of the bifunctional SAM is shown in SM-S3.

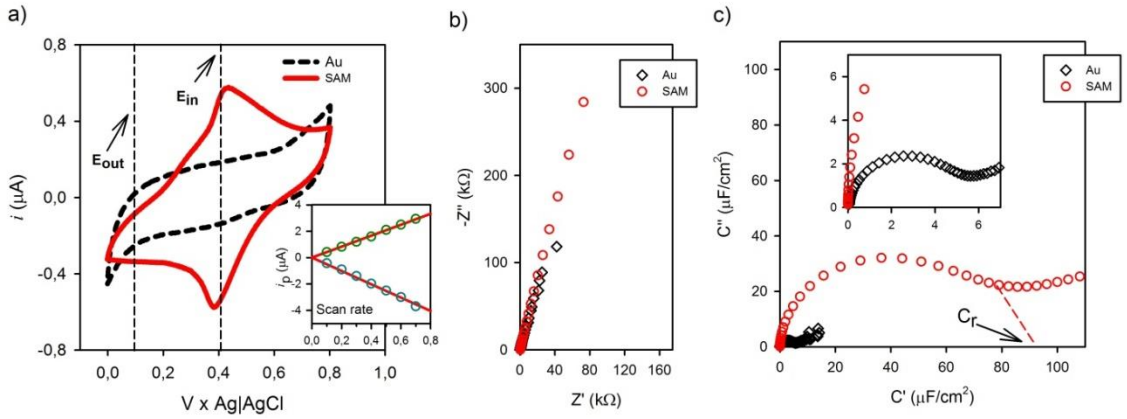

Figure 2. (a) CV obtained before (dashed black line) and after (red line) SAM formation. Conditions: 100 mM $NaClO_4$, potential range 0 to 0.8 V (x Ag|AgCl), scan rate 100 mV/s, 50 cycles. The 50th cycle is shown. The inset illustrates the linear dependence of current peak (anodic, i_{pa}; and cathodic, i_{pc}) in function of scan rate, from 100 to 700 mV/s. (b) Nyquist impedance plot obtained at E_{in} potential for bare gold (black diamond) and SAM (red circles). The impedance raw data can be converted to capacitance complex function, as shown in (c). The redox capacitance (C_r) can be estimated by semicircle diameter.[30, 38, 44] Conditions: measurements performed at E_{in} potential (≈ 400 mV x Ag|AgCl). AC perturbation amplitude of 10 mV. Frequency range from 100 KHz to 0.1 Hz (50 frequencies). Supporting electrolyte: 100 mM $NaClO_4$ aqueous solution.

The 11Fc surface coverage (Γ_{11Fc}) determined by integration of CV peaks (Figure 2a) is (1.8 ± 0.5) x 10^{-10} mol/cm^2. A similar value can be obtained using the linear dependence of the anodic or cathodic current peaks in function of scan rate (inset in Figure 2a), namely (1.4 ± 0.3) x 10^{-10} mol/cm^2. For comparison, an approximation based in the redox capacitance (using an approximation of the number of states at E_{in} energy level)[45] is (1.0 ± 0.1) x 10^{-10} mol/cm^2. The total SAM surface coverage (Γ_{SAM}) was evaluated by integrating the anodic peak (at ≈ -1.1 V) [46] (details in SM-S4) with a value of Γ_{SAM} = (5 ± 2) x 10^{-10} mol/cm^2, in line with expectations for films of this type. [47]

The impedance behavior of the mixed SAM was studied at two different potentials, *redox in* (E_{in} = 406 ± 4 mV) and *redox out* (E_{out} = 100 mV) as previously specified. *Redox in* potential corresponds to formal potential of the ferrocene couple, while *redox out* is only a charging potential, as illustrated in the vertical lines in Figure 2a (details of SAM impedance behavior can be found in SM-S3). From the Figure 2b, it is not possible to distinguish the differences in the impedance Nyquist plot (i.e. complex domain) from the data collected at E_{in} for bare gold and SAM modified surface. However, this problem can be overcome by converting the complex impedance raw data to capacitance. As can be seen, at the *redox in* potential for bare gold, only the capacitance value

related to double layer can be noted, 5 ± 1 μF/cm^2. Nevertheless, after SAM modification, the capacitance increases considerably (96 ± 14 μF/cm^2, associated with C_r from tethered redox SAM), evidencing the successful of gold electrode modification. The value found herein for C_r is consistent with previously reported one (≈ 100 μF/cm^2). [48]

After SAM formation and electrochemical assessment, the carboxylic groups present in the PEG-thiol were activated with EDC/NHS standard chemistry [49] for IgG antibody (anti-NS1) or antigen (NS1) receptor coupling. To block non-specific sites to avoid unspecific interaction, BSA at 1mg/mL diluted in PBS was used. During both steps it was possible to observe a specific decrease in C_r signal (Figure S5).[50] For more details, please refer to SM-S5.

After initial electrochemical characterization, the redox active receptive films were applied to target detection. Control receptive films are unresponsive to successive incubations in PBS or serum (demonstrating specificity and signal stability – see SM-S6 and SM-S7).

3.2 NS1 detection in PBS and diluted serum

For NS1 assay, the target protein was diluted in both PBS (pH 7.4) and diluted serum (1:4, sera:PBS) across a clinically relevant concentration range 1 to 5,000 ng/mL. [15] Aliquots of 50 μL of NS1 solution were used with an incubation time of 30 min. Figure 3 shows the capacitance Nyquist and Bode plots subsequently obtained. All measurements were performed at the E_{in} potential (note that at E_{out} the capacitance is unresponsive to target recognition). A decrease in redox capacitance signal (semicircle diameter) was observed, as expected. [30, 31, 51] It is worth noting that the relative response RR in function of target concentration (i.e. RR(%) = 100*(1/$C_{r,[NS1]}$-1/$C_{r,blank}$)/(1/$C_{r,blank}$), where $C_{r,[NS1]}$ is the redox capacitance signal for a specified NS1 concentration and $C_{r,blank}$ the signal of the blank) is Langmuir in form (details in SM-S8). The derived association affinity, K_a = (6 ± 2) x10^8 L/mol (K_D = (1.8 ± 0.6) nmol/L) is in the expected range. [30]

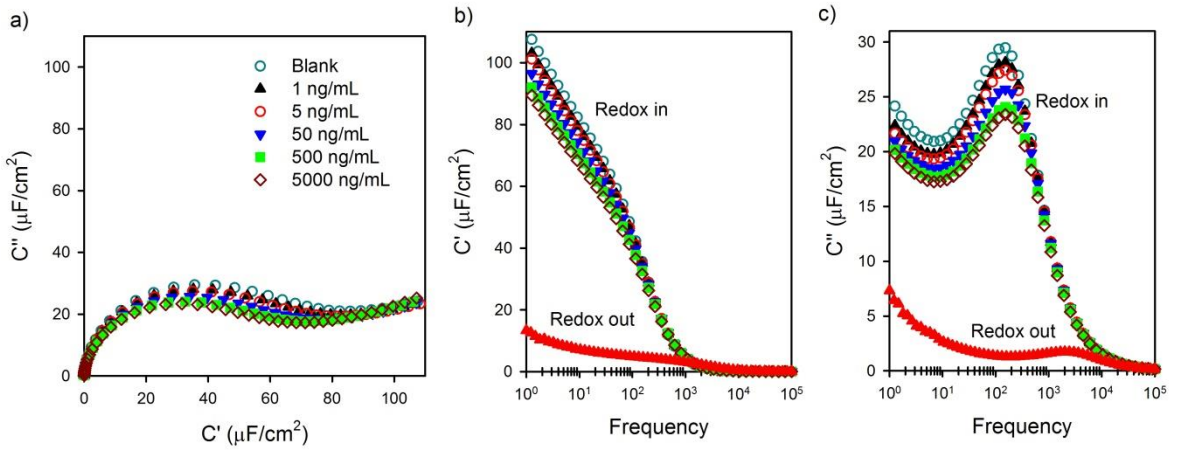

Figure 3. (a) Capacitive Nyquist plot obtained using different NS1 concentrations in PBS at E_{in}, which is possible to observe changes in C_r (semicircle diameter) in function of NS1 concentration. The real (b) and imaginary part of capacitance (c) are unresponsiveness at *redox out* potential E_{out} but at potential in E_{in}. Conditions: measurements performed at E_{in} potential (≈ 400 mV x Ag|AgCl). AC perturbation amplitude of 10 mV. Frequency range from 100 KHz to 0.1 Hz (50 frequencies). Supporting electrolyte: 100 mmol/L $NaClO_4$ aqueous solution.

From a constructed analytical curve (Figure 4) and derived analytical parameters (Table 1) using $1/C_r$ transduction, it is demonstrable that NS1 across a 1-5,000 ng/mL linear range is detectable with a sensitivity of 4.5% per decade. The associated LOD is 340 pg/mL, thus lower than reported by others using carbon nanotube-screen printed electrodes (12 ng/mL) [52] or by means of conventional faradaic impedance using redox probe in solution (3 ng/mL). [26] The reproducibility, measured herein by the average of the relative standard deviation (RSD) for all data points in the calibration curve ($RSD = sd/\overline{RR}$, where $\overline{RR}$ is the relative signal average for a certain target concentration, and sd the respective standard deviation) was 8.7%. As shown in Figure S9 (SM-S8), nonspecific responses (using diluted serum at 20%) were typically < 10% of the specific response.

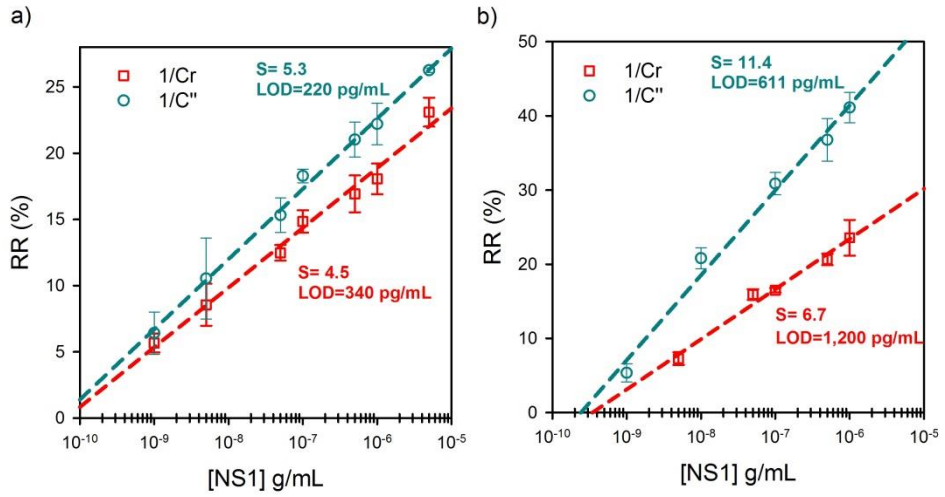

Figure 4. a) Analytical plot obtained for NS1 detection in PBS and (b) 20% serum. In red square, data obtained using $1/C_r$ as signal transduction, while in dark cyan circles for 1/C''. The sensibilities (S) and limits of detection (LOD) are mentioned in the plots. The correlation coefficient (i.e. Pearson, R) shown a strong positive linear dependence of the transduction signal in function of logarithm of NS1 concentration (R > 0.98), with correspondent coefficient of determination $R^2 > 0.98$.

The same approach was used to detect NS1 in diluted human serum at 20%. The standard curve is shown in Figure 4b (red squares) and the analytical parameters are summarised in Table 1. The methodology reported here presents a clinical relevant linear range of target concentration from 5-1,000 ng/mL,; NS1 is present in patients in concentrations from 40-2,000 ng/mL in primary and 10-2,000 ng/mL in secondary infections, respectively. In addition, the associated LOD of 1.2 ng/mL is a lower value than previously reported by traditional impedimetric approach.[26]

Table 1. Analytical parameters obtained for NS1 and IgG (anti-NS1) assays in PBS and diluted serum (1:4) by ECS ($1/C_r$) and 1/C'' (at 100 Hz). All measurements were carried out in triplicate.

Target	Approach	Assay condition	Linearity (ng/mL)	Sensitivity (% per decade)	LOD (pg/mL)	RSD (%)	R^2
NS1	$1/C_r$	PBS	1-5,000	4.5	340	8.7	0.987
		Diluted serum	5-1,000	6.7	1,200	7.0	0.983
	1/C''	PBS	1-5,000	5.3	220	11.3	0.995
		Diluted serum	1-1,000	11,4	611	9.4	0.987
IgG	$1/C_r$	PBS	1-1,000	6.3	231	7.0	0.975
		Diluted serum	10-1,000	16.9	6,100	5.0	0.965
	1/C''	PBS	1-1,000	6.3	393	3.4	0.995
		Diluted serum	10-1,000	15.7	9,500	4.2	0.961

3.3 IgG detection in PBS and diluted serum

In an extrapolation of this approach to surfaces constraining the NS1 antigen, anti-NS1 (IgG) assays can be developed. The resulting (Bode and Nyquist plots) are shown in SM-S9. Robust detection was possible across a log linear range of 1-1,000 ng/mL with a sensitivity of 6.3% per decade (Figure 5a) and LOD of 231 pg/mL. As shown in Figure S7 (SM-S7), the nonspecific responses are < 14% of specific response. In spiked dilute serum the relevant assay range is 10-1,000 ng/mL, with a LOD of 6,100 pg/mL.

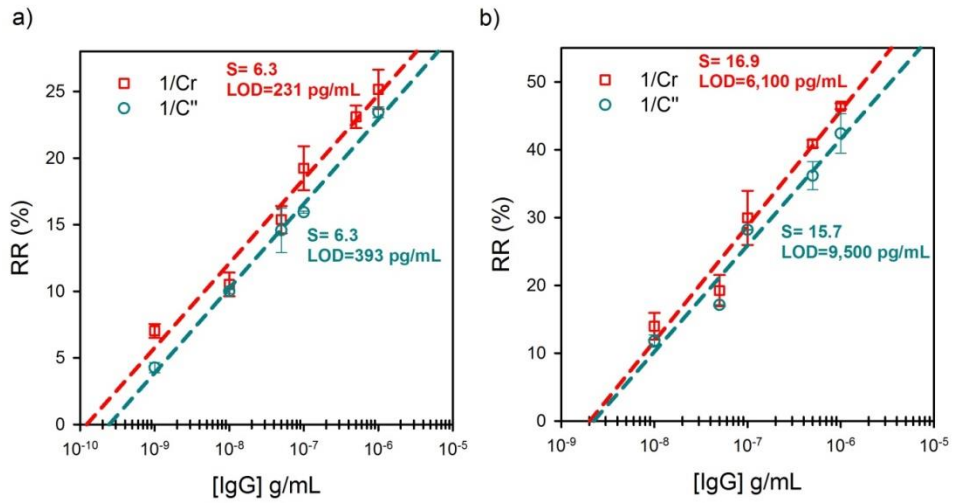

Figure 5. a) Representative analytical plots for IgG detection in PBS and (b) diluted serum at 20%. Data obtained using $1/C_r$ as signal transduction (red squares) and for $1/C''$ (dark cyan circles). The sensitivities (S) and limits of detection (LOD) are mentioned in the plots. The correlation coefficient (i.e. Pearson, R) shown a strong positive linear dependence of the transduction signal in function of logarithm of NS1 concentration ($R > 0.97$), with correspondent coefficient of determination $R^2 > 0.96$.

3.4 An alternative signal transduction for dengue detection: using 1/C'' immittance function

Although the label free EIS-derived redox capacitance approach is, then, both sensitive and analytically well-behaved in clinically-relevant immunorecognition, assay times can be dramatically reduced by moving to an immittance platform (with no change in the interface or the experiment otherwise). In previous work, we have identified the inverse of imaginary capacitance as an effective transducer signal of molecular recognition at higher analytical frequencies of a redox tagged interface (~ 7-100 Hz) when compared with purely capacitance analysis as described in the previous section. [32, 33] Accordingly, the optimized frequency found is of 100 Hz (Figure 6). The target-responsive data shown in Figure 6, for example, is acquired in <4 seconds at this frequency. The derived analytical data shown in Figures 4 and 5, and described in Table 1 (resolving likewise a

sensible association constant [K_a = (8 ± 2) x10^8 L/mol, details in SM-S8] confirms the validity of the approach.

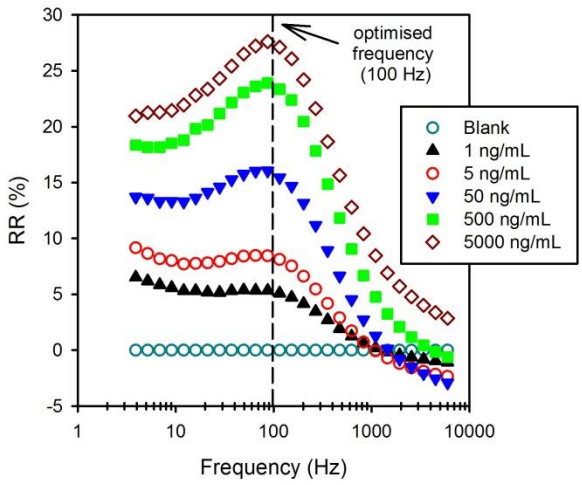

Figure 6. Example of 1/C'' immittance funcion obtained for NS1 detection in PBS. The optimised frequency, 100 Hz, corresponds to the sensitivest condition with $R^2 > 0.96$.

4. Conclusions

New methodologies for dengue detection are required since the standard methods typically suffer from long data acquisition time and the need for skilled personnel. Standard impedimetric approaches, although label free and sensitive, require an amplifying pre-doping of each analytical solution with redox probe and the acquisition of data across a broad range of frequencies prior fitting to an equivalent circuit representing the electrical response of the interface. Redox capacitive methods are cleaner, equivalently sensitive and, as presently shown, can be additionally improved in such a way that acquisition times are significantly reduced. Accordingly, here we demonstrated that both dengue primary antigen and antibodies are reliably assayed in serum across clinically relevant ranges in *a few seconds*. This study is readily extrapolated to include the real-time assessment of additional markers and represents, we believe, a practically relevant contribution to dengue diagnostics.

Acknowledgement

The authors thank Royal Society of Chemistry, FAPESP (Sao Paulo State Research Foundation) and CAPES.

References

1. Parkash, O. and R. Shueb, *Diagnosis of Dengue Infection Using Conventional and Biosensor Based Techniques.* Viruses, 2015. **7**(10): p. 2877.
2. Darwish, N.T., Y.B. Alias, and S.M. Khor, *An introduction to dengue-disease diagnostics.* TrAC Trends in Analytical Chemistry, 2015. **67**: p. 45-55.
3. Sinawang, Prima D., et al., *Electrochemical lateral flow immunosensor for detection and quantification of dengue NS1 protein.* Biosensors and Bioelectronics, 2016. **77**: p. 400-408.
4. Teles, F.S.R.R., *Biosensors and rapid diagnostic tests on the frontier between analytical and clinical chemistry for biomolecular diagnosis of dengue disease: A review.* Analytica Chimica Acta, 2011. **687**(1): p. 28-42.
5. Hales, S., et al., *Potential effect of population and climate changes on global distribution of dengue fever: an empirical model.* The Lancet, 2002. **360**(9336): p. 830-834.
6. *WHO (World Health Organization) - Dengue fever in Madeira, Portugal*. 2012; Available from: www.who.int/csr/don/2012_10_17/en/.
7. Gurugama, P., et al., *Dengue viral infections.* Indian Journal of Dermatology, 2010. **55**(1): p. 68-78.
8. Beatty, M.E., et al., *Best Practices in Dengue Surveillance: A Report from the Asia-Pacific and Americas Dengue Prevention Boards.* PLoS Neglected Tropical Diseases, 2010. **4**(11): p. e890.
9. Vijgen, L., et al., *Development of One-Step, Real-Time, Quantitative Reverse Transcriptase PCR Assays for Absolute Quantitation of Human Coronaviruses OC43 and 229E.* Journal of Clinical Microbiology, 2005. **43**(11): p. 5452-5456.
10. Freeman, W.M., S.J. Walker, and K.E. Vrana, *Quantitative RT-PCR: pitfalls and potential.* Biotechniques, 1999(26): p. 112-125.
11. Zhang, G.-J., et al., *Silicon nanowire biosensor for highly sensitive and rapid detection of Dengue virus.* Sensors and Actuators B: Chemical, 2010. **146**(1): p. 138-144.
12. Luo, X. and J.J. Davis, *Electrical biosensors and the label free detection of protein disease biomarkers.* Chemical Society Reviews, 2013. **42**(13): p. 5944-5962.
13. Santos, A., J.J. Davis, and P.R. Bueno, *Fundamentals and Applications of Impedimetric and Redox Capacitive Biosensors.* Journal of Analytical & Bioanalytical Techniques, 2014. **0**(0): p. -.
14. Lima, M.d.R.Q., et al., *Comparison of Three Commercially Available Dengue NS1 Antigen Capture Assays for Acute Diagnosis of Dengue in Brazil.* PLoS Neglected Tropical Diseases, 2010. **4**(7): p. e738.
15. Alcon, S., et al., *Enzyme-Linked Immunosorbent Assay Specific to Dengue Virus Type 1 Nonstructural Protein NS1 Reveals Circulation of the Antigen in the Blood during the Acute Phase of Disease in Patients Experiencing Primary or Secondary Infections.* Journal of Clinical Microbiology, 2002. **40**(2): p. 376-381.
16. Xu, H., et al., *Serotype 1-Specific Monoclonal Antibody-Based Antigen Capture Immunoassay for Detection of Circulating Nonstructural Protein NS1: Implications for Early Diagnosis and Serotyping of Dengue Virus Infections.* Journal of Clinical Microbiology, 2006. **44**(8): p. 2872-2878.
17. Allonso, D., et al., *Polyclonal antibodies against properly folded Dengue virus NS1 protein expressed in E. coli enable sensitive and early dengue diagnosis.* Journal of Virological Methods, 2011. **175**(1): p. 109-116.
18. Blacksell, S.D., et al., *Evaluation of six commercial point-of-care tests for diagnosis of acute dengue infections: The need for combining NS1 antigen and IgM/IgG antibody detection to achieve acceptable levels of accuracy.* Clinical and Vaccine Immunology, 2011. **18**(12): p. 2095-2101.

19. Wang, S.M. and S.D. Sekaran, *Evaluation of a Commercial SD Dengue Virus NS1 Antigen Capture Enzyme-Linked Immunosorbent Assay Kit for Early Diagnosis of Dengue Virus Infection.* Journal of Clinical Microbiology, 2010. **48**(8): p. 2793-2797.
20. Wang, S.M. and S.D. Sekaran, *Early Diagnosis of Dengue Infection Using a Commercial Dengue Duo Rapid Test Kit for the Detection of NS1, IGM, and IGG.* The American Journal of Tropical Medicine and Hygiene, 2010. **83**(3): p. 690-695.
21. Lima, J.R.C., et al., *Interpretation of the presence of IgM and IgG antibodies in a rapid test for dengue: analysis of dengue antibody prevalence in Fortaleza City in the 20th year of the epidemic.* Revista da Sociedade Brasileira de Medicina Tropical, 2012. **45**: p. 163-167.
22. Wong, W.R., et al., *Detection of dengue NS1 antigen using long-range surface plasmon waveguides.* Biosensors and Bioelectronics, 2016. **78**: p. 132-139.
23. TAI, D.-F., et al., *Artificial receptors in serologic tests for the early diagnosis of dengue virus infection.* Clinical Chemistry, 2006. **52**(n. 8): p. 1486-1491.
24. Su, C.-C., et al., *Development of immunochips for the detection of dengue viral antigens.* Analytica Chimica Acta, 2003. **479**(2): p. 117-123.
25. Oliveira, M.D.L., M.T.S. Correia, and F.B. Diniz, *Concanavalin A and polyvinyl butyral use as a potential dengue electrochemical biosensor.* Biosensors and Bioelectronics, 2009. **25**(4): p. 728-732.
26. Cecchetto, J., et al., *An impedimetric biosensor to test neat serum for dengue diagnosis.* Sensors and Actuators B: Chemical, 2015. **213**(0): p. 150-154.
27. Darwish, N.T., et al., *Electrochemical Immunosensor Based on Antibody-Nanoparticle Hybrid for Specific Detection of the Dengue Virus NS1 Biomarker.* Journal of The Electrochemical Society, 2016. **163**(3): p. B19-B25.
28. Cecchetto, J., et al., *The capacitive sensing of NS1 Flavivirus biomarker.* Biosensors and Bioelectronics, 2017. **87**: p. 949-956.
29. Lisdat, F. and D. Schäfer, *The use of electrochemical impedance spectroscopy for biosensing.* Analytical and Bioanalytical Chemistry, 2008. **391**(5): p. 1555-1567.
30. Fernandes, F.C.B., et al., *Comparing label free electrochemical impedimetric and capacitive biosensing architectures.* Biosensors and Bioelectronics, 2014. **57**(0): p. 96-102.
31. Fernandes, F.C.B., et al., *Label free redox capacitive biosensing.* Biosensors and Bioelectronics, 2013. **50**(0): p. 437-440.
32. Santos, A. and P.R. Bueno, *Glycoprotein assay based on the optimized immittance signal of a redox tagged and lectin-based receptive interface.* Biosensors and Bioelectronics, 2016. **83**: p. 368-378.
33. Bedatty Fernandes, F.C., et al., *Optimized Diagnostic Assays Based on Redox Tagged Bioreceptive Interfaces.* Analytical Chemistry, 2015. **87**(24): p. 12137-12144.
34. Patil, A.V., et al., *Immittance Electroanalysis in Diagnostics.* Analytical Chemistry, 2015. **87**(2): p. 944-950.
35. Alcantar, N.A., E.S. Aydil, and J.N. Israelachvili, *Polyethylene glycol–coated biocompatible surfaces.* Journal of Biomedical Materials Research, 2000. **51**(3): p. 343-351.
36. Marques, S.M., et al., *Sensitive label-free electron chemical capacitive signal transduction for D-dimer electroanalysis.* Electrochimica Acta, 2015. **182**: p. 946-952.
37. Goes, M.S., et al., *A Dielectric Model of Self-Assembled Monolayer Interfaces by Capacitive Spectroscopy.* Langmuir, 2012. **28**(25): p. 9689-9699.
38. Bueno, P.R., G. Mizzon, and J.J. Davis, *Capacitance Spectroscopy: A Versatile Approach To Resolving the Redox Density of States and Kinetics in Redox-Active Self-Assembled Monolayers.* Journal of Physical Chemistry B, 2012. **116**(30): p. 8822-8829.
39. Piccoli, J.P., et al., *The self-assembly of redox active peptides: Synthesis and electrochemical capacitive behavior.* Peptide Science, 2016. **106**(3): p. 357-367.

40. Walczak, M.M., et al., *Reductive desorption of alkanethiolate monolayers at gold: a measure of surface coverage.* Langmuir, 1991. **7**(11): p. 2687-2693.
41. Eckermann, A.L., et al., *Electrochemistry of redox-active self-assembled monolayers.* Coord Chem Rev, 2010. **254**(15-16): p. 1769-1802.
42. Long, G.L. and J.D. Winefordner, Analytical Chemistry, 1983. **55**(7): p. 712-724.
43. Eckermann, A.L., et al., *Electrochemistry of redox-active self-assembled monolayers.* Coordination Chemistry Reviews, 2010. **254**(15–16): p. 1769-1802.
44. Bueno, P.R., G.T. Feliciano, and J.J. Davis, *Capacitance spectroscopy and density functional theory.* Physical Chemistry Chemical Physics, 2015. **17**(14): p. 9375-9382.
45. Bueno, P.R. and J.J. Davis, *Elucidating redox level dispersion and local dielectric effects within electroactive molecular films.* Anal. Chem., 2014. **86**(4): p. 1977-2004.
46. Pensa, E., et al., *New insights into the electrochemical desorption of alkanethiol SAMs on gold.* Physical chemistry chemical physics : PCCP, 2012. **14**(35): p. 12355-12367.
47. Love, J.C., et al., *Self-Assembled Monolayers of Thiolates on Metals as a Form of Nanotechnology.* Chemical Reviews, 2005. **105**(4): p. 1103-1170.
48. Bueno, P.R., F. Fabregat-Santiago, and J.J. Davis, *Elucidating Capacitance and Resistance Terms in Confined Electroactive Molecular Layers.* Analytical Chemistry, 2013. **85**(1): p. 411-417.
49. Fischer, M.J., *Amine Coupling Through EDC/NHS: A Practical Approach*, in *Surface Plasmon Resonance*. 2010. p. 55-73.
50. Lehr, J., et al., *Label-free Capacitive Diagnostics: Exploiting Local Redox Probe State Occupancy.* Analytical Chemistry, 2014. **86**(5): p. 2559-2564.
51. Santos, A., et al., *Impedance-derived electrochemical capacitance spectroscopy for the evaluation of lectin–glycoprotein binding affinity.* Biosensors and Bioelectronics, 2014. **62**: p. 102-105.
52. Dias, A.C.M.S., et al., *A sensor tip based on carbon nanotube-ink printed electrode for the dengue virus NS1 protein.* Biosensors and Bioelectronics, 2013. **44**: p. 216-221.